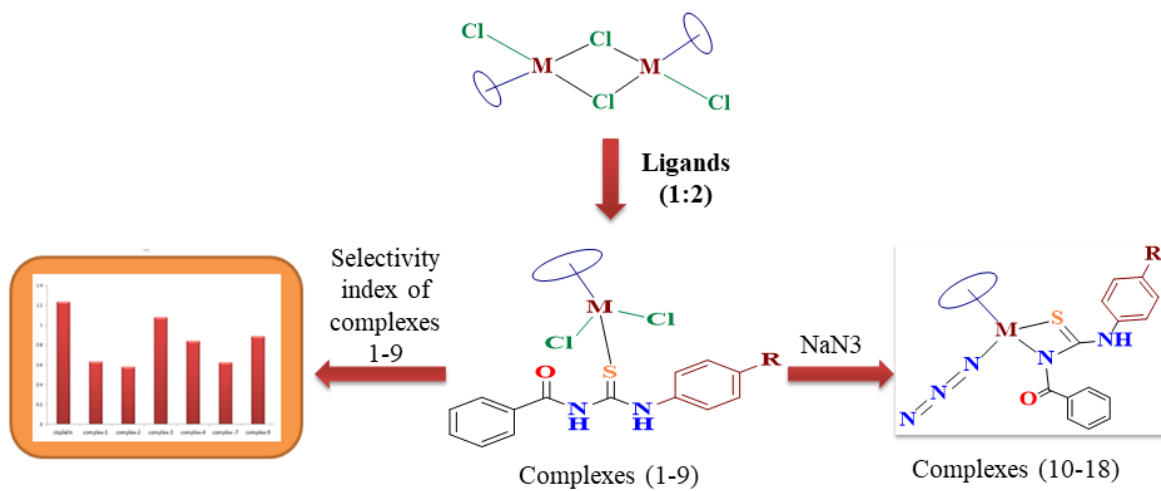




14 **Graphical Abstract**

15



16

17

18 **Abstract**

19           The reaction of [(*p*-cymene)RuCl<sub>2</sub>]<sub>2</sub> and [Cp\**M*Cl<sub>2</sub>]<sub>2</sub> (*M* = Rh/Ir) metal precursors with  
20 aroylthiourea ligands (L1-L3) yielded a series of neutral mono-dentate complexes **1-9**. The  
21 neutral mono-dentate coordination of aroylthiourea with metals *via* S atom was confirmed by  
22 single crystal X-ray diffraction study. Further reaction of mono-dentate complexes **1-9** with  
23 excess NaN<sub>3</sub> in polar solvent resulted in the formation of highly strained four member ring  $\kappa^2_{(N,S)}$   
24 azido complexes **10-18**. Further these complexes were treated with activated alkynes to isolate  
25 triazole complexes, but unfortunately the reaction was unsuccessful. All these complexes were  
26 fully characterized by various spectroscopic techniques. The molecular structures of the  
27 representative complexes have been determined by single crystal X-ray diffraction studies. The  
28 molecular structures of the complexes revealed typical piano stool geometry around the metal  
29 center. The chemosensitivity activities of the complexes **1-9** evaluated against the cancer cell line  
30 HCT-116 (human colorectal carcinoma) and ARPE-19 (human retinal epithelial cells) cell line.  
31 Of these, complex **3** was the most potent and whilst its potency was less than cisplatin, its  
32 selectivity for cancer as opposed to non-cancer cell lines *in vitro* was comparable to cisplatin.

33 -----

34 **Keywords:** Ruthenium, rhodium, iridium, thiourea, chemosensitivity.

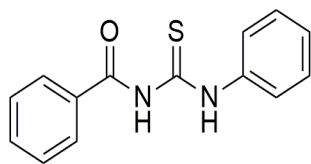
## 35 **Introduction**

36           The discovery of the anticancer activity of cisplatin by Rosenberg led to the development  
37 of numerous metal-based compounds as potential drugs in the war on cancer. Platinum based  
38 drugs namely cisplatin, carboplatin and oxaliplatin are among the most effective anticancer  
39 drugs, which have been widely used [1-2]. However, some drawback such as neurotoxicity,  
40 nephrotoxicity, intrinsic resistance of some tumors and dose-limiting side effects has limited the  
41 use of the platinum diammine compounds, cisplatin and carboplatin [3]. In order to overcome  
42 these obstacles and develop safer and more effective remedial agents, intensive efforts have been  
43 devoted toward the design and pharmacological evaluation of other metal-based drugs [4-5]. In  
44 the search for anticancer agents containing metals other than platinum, ruthenium compounds  
45 turned out to be the most promising ones, largely because the ligand exchange kinetics of metal  
46 complexes in aqueous solution, (which seem to be crucial for the anticancer activity) is favored  
47 [6-7]. Ruthenium has therefore been considered to be an attractive alternative to platinum  
48 particularly as many ruthenium compounds are not very toxic and some ruthenium compounds  
49 have been shown to be quite selective for cancer cells [8-9]. Following the first in vitro study of  
50 arene ruthenium compounds as anticancer agents by *Tocher et al.*, in 1992, the field of antitumor  
51 and anti-metastatic arene ruthenium complexes has received considerable attention and several  
52 anticancer ruthenium complexes, [NAMI-A](#) and KP1019 exerted potent activities against  
53 numerous tumor cells [10, 11]. Furthermore, (*p*-cymene)Ru complexes like [RuCl<sub>2</sub>(*p*-  
54 cymene)(pta)] (RAPTA-C), show attracted considerable attention due to their promising anti-  
55 metastatic activity in vivo activities on the inhibition of metastasis growth, together with a high  
56 selectivity and low general toxicity [12]. In addition Cp\*rhodium and Cp\*iridium complexes  
57 have also attracted considerable current interest due to their potential anticancer activity [13-17].

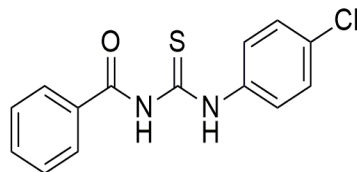
58 Some of the  $d^6$  metal complexes of ruthenium (II) [18, 19], rhodium (III) [17] and iridium (III)  
59 [20, 21] have also been found to inhibit the tumors by their selective interactions with cellular  
60 biomolecules.

61 Aroylthiourea ligands have been noted for their versatility because they are able to  
62 coordinate to a wide range of metal ions as neutral, monobasic or dibasic ligands [22]. N, N-  
63 Disubstituted thiourea being versatile precursors has been subjected to a various structural  
64 modifications in order to prepare a variety of their derivatives with different biological aspects.  
65 Some of N, N-disubstituted thiourea themselves are remarkable owing to their pharmacological  
66 and biological importance [23]. In vitro studies have revealed that various classes of thiourea are  
67 useful as potential antiviral, antibacterial, antifungal, antitubercular, anti-inflammatory,  
68 herbicidal, insecticidal and anticancer agent [24-31]. Thiourea may react with other reagents  
69 having different functionalities to yield active compounds of biological significance. The  
70 biological importance of both aroylthiourea and the ruthenium-arene unit has prompted us to  
71 explore the biological applications of ruthenium-arene complexes containing aroylthiourea  
72 ligand. Herein we describe the synthesis of  $[(arene)MCl_2]$  core complexes containing S donor  
73 aroylthiourea ligand and evaluate their cytotoxic properties and non-cancer cells in vitro.

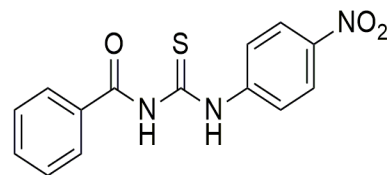
74 In recent years, we have reported many organometallic complexes including half-  
75 sandwich platinum group metal complexes containing thiourea ligands [32-34]. Recently we  
76 have also reported the synthesis of strained complexes of arene  $d^6$  metals containing  
77 benzoylthiourea ligand [35]. In continuation of our previous work, herein we report the  
78 synthesis of neutral mono-dentate half-sandwich arene ruthenium, rhodium and iridium  
79 complexes containing aroylthiourea derivatives and their reactivity with azide. Ligands used in  
80 this study are shown in (Chart 1).



L1



L2



L3

81

82

**Chart 1.** Ligands used in present study.

## 83 2. Experimental Section

### 84 2.1. Physical methods and materials

85 The reagents used were of commercial quality and used without further purification.

86 Benzoyl chloride, ammonium thiocyanate, aniline and 4-chloroaniline were purchased from

87 Sigma-Aldrich. 4-Nitroaniline was obtained from Alfa Aesar. The syntheses of all the complexes

88 were performed without using any inert atmosphere. All solvents used for syntheses were dried

89 and distilled prior to use according to standard procedures. Starting compounds [(*p*-

90 cymene)RuCl<sub>2</sub>]<sub>2</sub> were prepared according to reported method [36], and [Cp\**M*Cl<sub>2</sub>]<sub>2</sub> (*M* = Rh/Ir)

91 complexes were synthesized by using an Anton Paar monowave 50 synthesizer in 10 mL

92 microwave vials equipped with magnetic stirring bars which is described in experimental

93 section. Infrared (IR) spectra (400-4000 cm<sup>-1</sup>) were recorded on a Perkin-Elmer 983

94 spectrophotometer with compounds being dispersed as KBr discs. <sup>1</sup>H NMR spectra were

95 recorded on a Bruker Avance II 400 MHz instrument using CDCl<sub>3</sub> as solvent chemical shifts

96 were referenced to TMS. Mass spectra were obtained from Waters ZQ 4000 mass spectrometer

97 by ESI method using acetonitrile as solvent. Absorption spectra were recorded on a Perkin-Elmer

98 Lambda 25 UV/Vis spectrophotometer in the range of 200-600 nm at room temperature in

99 acetonitrile. Elemental analyses of the complexes were performed on a Perkin-Elmer 2400 CHN

100 analyzer.

101

## 102 *2.2. Single-crystal X-ray structures analyses*

103           The crystal of complexes **2**, **3**, **4**, **5**, **6**, **7**, **8**, **10**, **16** and **17** were obtained by slow diffusion  
104 of hexane over dichloromethane solution of the corresponding complexes. Single crystal X-ray  
105 diffraction measurement was carried out on an Oxford Diffraction Xcalibur Eos Gemini  
106 diffractometer at 293 K using graphite monochromated Mo-K $\alpha$  radiation ( $\lambda = 0.71073 \text{ \AA}$ ). The  
107 strategy for the data collection was evaluated using the CrysAlisPro CCD software. Crystal data  
108 were collected by standard “phi-omega scan” techniques and were scaled and reduced using  
109 CrysAlisPro RED software. The structures were solved by direct methods using SHELXS-97  
110 and refined by full-matrix least squares with SHELXL-97 refining on F<sup>2</sup> [37]. The positions of  
111 all the atoms were obtained by direct methods. Metal atoms in the complex were located from  
112 the E-maps and non-hydrogen atoms were refined anisotropically. The hydrogen atoms bound to  
113 the carbon were placed in geometrically constrained positions and refined with isotropic  
114 temperature factors, generally 1.2U<sub>eq</sub> of their parent atoms. Crystallographic and structure  
115 refinement parameters for the complexes are summarized in [Table S1](#) and [Table S2](#), and selected  
116 bond lengths and bond angles are presented in [Table 1](#) and [Table 2](#). Figures (1-7) were drawn  
117 with ORTEP3 [38].

## 118 *2.3. Cell line testing*

119           The human colorectal carcinoma cell line HCT116 p53 +/+ cells and the non-cancer  
120 human retinal epithelial cell line ARPE-19 were obtained from the American Type Culture  
121 Collection. Antiproliferative activity of the compounds was evaluated using the standard MTT  
122 (3-(4,5-Dimethylthiazol-2-yl)-2,5-diphenyltetrazolium bromide) cellular viability assay as  
123 described elsewhere [39]. Briefly, cells were seeded into 96 well plates at  $1.5 \times 10^3$  cells per well

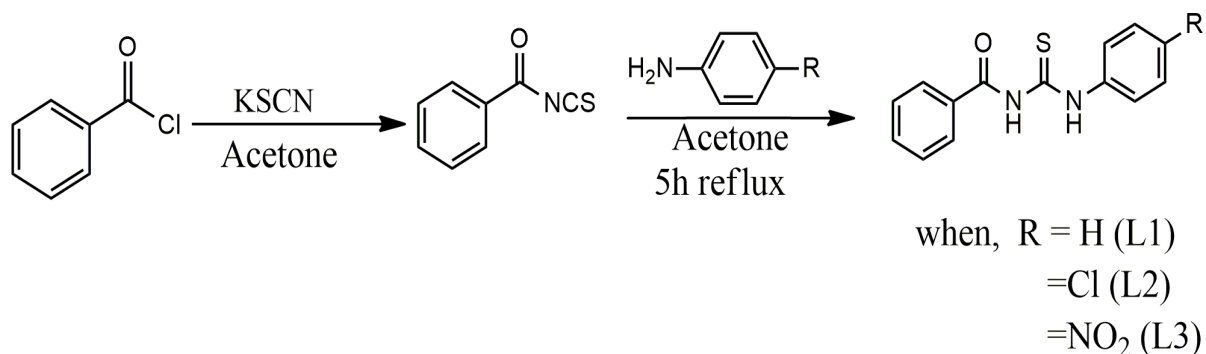
124 and incubated for 24 hours at 37 °C in an atmosphere of 5% CO<sub>2</sub> prior to drug exposure. Stock  
125 solution was freshly prepared by dissolving each of the compounds in dimethylsulphoxide  
126 (DMSO) at a concentration of 100 mM, which was subsequently diluted with medium to obtain  
127 drug solutions ranging from 0.5 to 100 µM. The final DMSO concentration was 0.1% (v/v),  
128 which is nontoxic to cells. Cisplatin was dissolved in phosphate buffered saline at a stock  
129 concentration of 25 mM. The cells were exposed to a range of drug concentrations for 96 hours  
130 and cell survival was determined using the MTT assay. Following drug exposure 20 µL of MTT  
131 (0.5 mg/ml) in phosphate buffered saline was added to each well and it was further incubated at  
132 37°C for 4 hours in an atmosphere containing 5% CO<sub>2</sub>. The solution was then removed and the  
133 formed formazan crystals was dissolved in 150 µM DMSO. The absorbance of the resulting  
134 solution was recorded at 550nm using an ELISA spectrophotometer. The percentage of cell  
135 survival was calculated by dividing the true absorbance of treated cell by the true absorbance for  
136 controls (exposed to 0.1% DMSO). The IC<sub>50</sub> values were determined from plots of percentage  
137 survival against drug concentration. Each experiment was performed in triplicate and a mean  
138 value obtained and stated as IC<sub>50</sub> (µM) ± SD. To compare the response of non-cancer cells to  
139 cancer cells, the selectivity index (SI) was also calculated which is defined as the IC<sub>50</sub> for ARPE-  
140 19 cells divided by the IC<sub>50</sub> for HCT-116 cells. Values >1 indicate that complexes have selective  
141 activity against cancer compared to non-cancer cells in vitro.

#### 142 2.4. *General procedure for synthesis of ligands (L1-L3)*

143 Freshly prepared benzoyl isothiocyanate was mixed in a 1:1 molar ratio with the desired  
144 substituted aniline in dry acetone and the mixture was reflux at 50 °C for about 5 h. On cooling,  
145 the reaction mixture was slowly poured into acidified (pH 4–5) chilled water and stirred well

146 with a glass rod. The solid, which formed, was separated by filtration and the precipitates were  
147 washed with distilled water and dried at room temperature (Scheme 1).

148



149

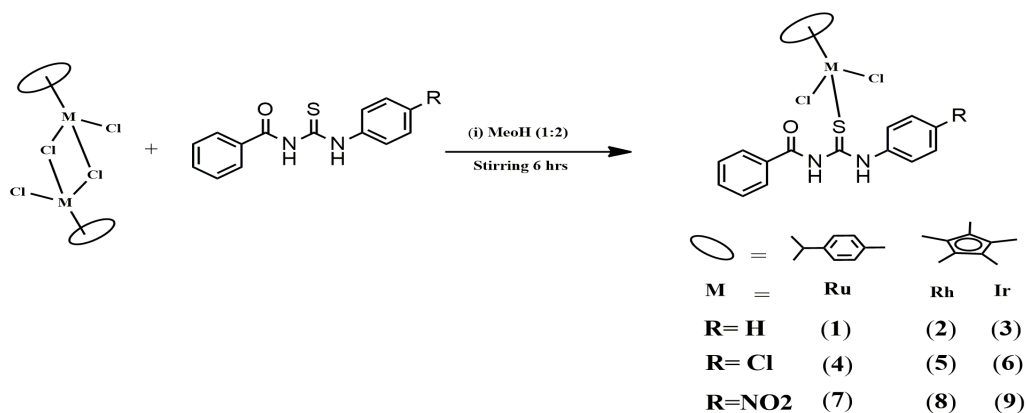
150 **Scheme 1.** Synthesis of thiourea ligands (**L1-L3**)

151 *2.5. General preparation of [Cp\**M*Cl<sub>2</sub>]<sub>2</sub> (M = Rh/Ir)*

152 RhCl<sub>3</sub>·3H<sub>2</sub>O (0.50 g) or IrCl<sub>3</sub>·3H<sub>2</sub>O (0.50 g) was dissolved in MeOH (3 ml) in a mono-  
153 wave vial, and 0.5 ml of 1,2,3,4,5-pentamethylcyclopentadiene was added. The vial was placed  
154 in the mono-wave instrument the pressure was set at 20 bar and heated to 110 °C with stirring for  
155 45 minutes. After cooling to room temperature, the vial was opened. After short vigorous  
156 shaking, the precipitate was allowed to settle down, and the solvent was decanted. The  
157 microcrystalline product was isolated, washed with diethyl ether (3×5 ml), and dried under  
158 vacuum. Yield: (88%)

159 *2.6. General procedure for synthesis of neutral complexes (1-9)*

160 A mixture of starting metal precursor (0.1 mmol) and ligands (0.2 mmol) were dissolved  
161 in dry methanol (10 ml) and stirred at room temperature for 6 hours (Scheme-2). A yellow  
162 colored compound precipitated out from the reaction mixture. The precipitate was filtered,  
163 washed with cold methanol (5 ml) and diethyl ether (2 x 5 ml) and dried in vacuum.



164

165

**Scheme 2.** Schematic representation for the synthesis of complexes (1-9)

166

2.6.1. [(*p*-cymene)Ru( $\kappa^1_{(S)}$ -L1)Cl<sub>2</sub>] (**1**)

167

Yield: (68%); IR (KBr, cm<sup>-1</sup>): 3068-3440  $\nu_{(N-H)}$ , 1665  $\nu_{(C=O)}$ , 1213  $\nu_{(C=S)}$ ; <sup>1</sup>H NMR (400 MHz,

168

CDCl<sub>3</sub>, ppm): 12.91 (s, 1H, NH), 11.29 (s, 1H, NH), 8.22 (d, 2H, *J* = 8 Hz), 7.82 (d, 1H, *J* = 8

169

Hz), 7.49 (t, 1H, *J* = 8 Hz), 7.38-7.45 (m, 5H), 7.32 (t, 1H, *J* = 8 Hz), 5.33 (d, 2H, *J* = 8 Hz), 5.18

170

(d, 2H, *J* = 8 Hz) 2.82-2.93 (sept, 1H), 2.17 (s, 3H), 1.23 (d, 6H, *J* = 8 Hz); ESI-MS (*m/z*):

171

490.96 [M-2Cl]<sup>+</sup>; UV-Vis { Acetonitrile,  $\lambda_{max}$  nm ( $\epsilon/10^{-4}$  M<sup>-1</sup> cm<sup>-1</sup>): 255 (0.95), 364(0.12). **Anal.**

172

**Calc. for C<sub>24</sub>H<sub>26</sub>Cl<sub>2</sub>N<sub>2</sub>ORuS (562.52): C, 51.24; H, 4.66; N, 4.98. Found: C, 51.30; H, 4.63; N,**

173

**4.76.**

174

2.6.2. [Cp\**Rh*( $\kappa^1_{(S)}$ -L1)Cl<sub>2</sub>](**2**)

175

Yield: (72%); IR (KBr, cm<sup>-1</sup>): 3052-3447  $\nu_{(N-H)}$ , 1667  $\nu_{(C=O)}$ , 1210  $\nu_{(C=S)}$ ; <sup>1</sup>H NMR (400 MHz,

176

CDCl<sub>3</sub>, ppm): 13.06 (s, 1H, NH), 11.40 (s, 1H, NH), 8.27 (d, 2H, *J* = 8 Hz), 7.48-7.52 (m, 3H),

177

7.43 (d, 2H, *J* = 12 Hz), 7.41 (d, 1H, *J* = 4 Hz), 7.38 (d, 2H, *J* = 12 Hz), 7.29 (t, 1H, *J* = 12 Hz),

178

1.56 (s, 15H). ESI-MS (*m/z*): 493.02 [M-2Cl]<sup>+</sup>; UV-Vis {Acetonitrile,  $\lambda_{max}$  nm ( $\epsilon/10^{-4}$  M<sup>-1</sup> cm<sup>-1</sup>),

179

<sup>1</sup>): 263 (0.45). **Anal. Calc. for C<sub>24</sub>H<sub>27</sub>Cl<sub>2</sub>N<sub>2</sub>ORhS (565.36): C, 50.99; H, 4.81; N, 4.95. Found:**

180

**C, 51.01; H, 4.75; N, 5.15.**

181

2.6.3. [Cp\**Ir*( $\kappa^1_{(S)}$ -L1)Cl<sub>2</sub>](**3**)

182 Yield: (56%); IR (KBr,  $\text{cm}^{-1}$ ): 3054-3436  $\nu_{(\text{N-H})}$ , 1668  $\nu_{(\text{C=O})}$ , 1211  $\nu_{(\text{C=S})}$ ;  $^1\text{H}$  NMR (400 MHz,  
183  $\text{CDCl}_3$ , ppm): 13.06 (s, 1H, NH), 11.84 (s, 1H, NH), 8.41 (d, 2H,  $J = 8$  Hz), 7.60 (t, 1H,  $J = 8$   
184 Hz), 7.51-7.56 (m, 4H), 7.45 (t, 2H,  $J = 8$  Hz), 7.37 (t, 1H,  $J = 8$  Hz), 1.65 (s, 15H); ESI-MS  
185 (m/z): 581.01  $[\text{M}-2\text{Cl}]^+$ ; UV-Vis {Acetonitrile,  $\lambda_{\text{max}}$  nm ( $\epsilon/10^{-4}$   $\text{M}^{-1}$   $\text{cm}^{-1}$ ): 257(0.30), 350  
186 (0.067). Anal. Calc. for  $\text{C}_{24}\text{H}_{27}\text{Cl}_2\text{IrN}_2\text{OS}$  (654.67): C, 44.03; H, 4.16; N, 4.28. Found: C, 44.01;  
187 H, 4.29; N, 4.05.

#### 188 2.6.4. $[(p\text{-cymene})\text{Ru}(\kappa^1_{(\text{S})}\text{-L2})\text{Cl}_2](\mathbf{4})$

189 Yield: (73%); IR (KBr,  $\text{cm}^{-1}$ ): 3171-3350  $\nu_{(\text{N-H})}$ , 1657  $\nu_{(\text{C=O})}$ , 1206  $\nu_{(\text{C=S})}$ ;  $^1\text{H}$  NMR (400 MHz,  
190  $\text{CDCl}_3$ , ppm): 12.96 (s, 1H, NH), 11.36 (s, 1H, NH), 8.27 (d, 2H,  $J = 4$  Hz), 7.57 (t, 1H,  $J = 8$   
191 Hz), 7.50-7.44 (m, 6H), 5.41 (d, 2H,  $J = 8$  Hz), 5.26 (d, 2H,  $J = 8$  Hz), 2.91-2.98 (sept, 1H), 2.24  
192 (s, 3H), 1.30 (d, 6H,  $J = 8$  Hz); ESI-MS (m/z):  $[\text{M}-2\text{Cl}]^+$ ; UV-Vis {Acetonitrile,  $\lambda_{\text{max}}$  nm ( $\epsilon/10^{-4}$   
193  $\text{M}^{-1}$   $\text{cm}^{-1}$ ): 260 (0.73), 357 (0.10). Anal. Calc. for  $\text{C}_{24}\text{H}_{25}\text{Cl}_3\text{N}_2\text{ORuS}$  (596.96): C, 48.29; H,  
194 4.22; N, 4.69. Found: C, 48.33; H, 4.22; N, 4.77,

#### 195 2.6.5. $[\text{Cp}^*\text{Rh}(\kappa^1_{(\text{S})}\text{-L2})\text{Cl}_2](\mathbf{5})$

196 Yield: (81%); IR (KBr,  $\text{cm}^{-1}$ ): 3128-3434  $\nu_{(\text{N-H})}$ , 1665  $\nu_{(\text{C=O})}$ , 1211  $\nu_{(\text{C=S})}$ ;  $^1\text{H}$  NMR (400 MHz,  
197  $\text{CDCl}_3$ , ppm): 13.10 (s, 1H, NH), 11.50 (s, 1H, NH), 8.34 (d, 2H,  $J = 8$  Hz), 7.58 (t, 1H,  $J = 8$   
198 Hz), 7.49-7.53 (m, 4H,  $J = 8$  Hz), 7.43 (d, 2H,  $J = 8$  Hz), 1.75 (s, 15H); ESI-MS (m/z): 527.19  
199  $[\text{M}-2\text{Cl}]^+$ ; UV-Vis {Acetonitrile,  $\lambda_{\text{max}}$  nm ( $\epsilon/10^{-4}$   $\text{M}^{-1}$   $\text{cm}^{-1}$ ): 264 (0.38). Anal. Calc. for  
200  $\text{C}_{24}\text{H}_{26}\text{Cl}_3\text{N}_2\text{ORhS}$  (599.81): C, 48.06; H, 4.37; N, 4.67. Found: C, 47.85; H, 4.42; N, 4.45.

#### 201 2.6.6. $[\text{Cp}^*\text{Ir}(\kappa^1_{(\text{S})}\text{-L2})\text{Cl}_2](\mathbf{6})$

202 Yield: (73%); IR (KBr,  $\text{cm}^{-1}$ ): 3056-3430  $\nu_{(\text{N-H})}$ , 1669  $\nu_{(\text{C=O})}$ , 1204  $\nu_{(\text{C=S})}$ ;  $^1\text{H}$  NMR (400 MHz,  
203  $\text{CDCl}_3$ , ppm): 13.06 (s, 1H, NH), 11.88 (s, 1H, NH), 8.40 (d, 2H,  $J = 8$  Hz), 7.60 (t, 1H,  $J = 8$   
204 Hz), 7.47-7.55 (m,  $J = 8$  Hz, 4H), 7.44 (dd, 2H,  $J = 8$  Hz), 1.61 (s, 15H); (m/z) ESI-MS:

205 617.22 [M-2Cl]<sup>+</sup>; UV-Vis {Acetonitrile,  $\lambda_{\max}$  nm ( $\epsilon/10^{-4}$  M<sup>-1</sup> cm<sup>-1</sup>): 271(0.83), 355 (0.078).  
206 Anal. Calc. for C<sub>24</sub>H<sub>26</sub>Cl<sub>3</sub>IrN<sub>2</sub>OS (689.12): C, 41.83; H, 3.80; N, 4.07. Found: C, 41.84; H, 3.82;  
207 N, 4.15.

208 2.6.7. [(*p*-cymene)Ru( $\kappa^1$ <sub>(S)</sub>-L3)Cl<sub>2</sub>] (7)

209 Yield: (84%); IR (KBr, cm<sup>-1</sup>): 3164-3467  $\nu$ (N-H), 1659  $\nu$ (C=O), 1209  $\nu$ (C=S); <sup>1</sup>H NMR (400 MHz,  
210 CDCl<sub>3</sub>, ppm): 13.41 (s, 1H, NH), 11.49 (s, 1H, NH), 8.35 (d, 2H, *J* = 8 Hz), 8.27 (d, 2H, *J* = 8  
211 Hz), 7.77 (d, 2H, *J* = 8 Hz), 7.58 (t, 1H, *J* = 4 Hz), 7.50 (t, 2H, *J* = 8 Hz), 5.45 (d, 2H, *J* = 8 Hz),  
212 5.30 (d, 2H, *J* = 8 Hz), 2.91-3.02 (sept, 1H), 2.27 (s, 3H), 1.31 (d, 6H); ESI-MS (m/z): 535.13  
213 [M-2Cl]<sup>+</sup>; UV-Vis {Acetonitrile,  $\lambda_{\max}$  nm ( $\epsilon/10^{-4}$  M<sup>-1</sup> cm<sup>-1</sup>): 281 (0.40), 347 (0.22). Anal. Calc.  
214 for C<sub>24</sub>H<sub>25</sub>Cl<sub>2</sub>N<sub>3</sub>O<sub>3</sub>RuS (607.51): C, 47.45; H, 4.15; N, 6.92. Found: C, 47.43; H, 4.16; N, 6.74.

215 2.6.8. [Cp\*Rh( $\kappa^1$ <sub>(S)</sub>-L3)Cl<sub>2</sub>] (8)

216 Yield: (75%); IR (KBr, cm<sup>-1</sup>): 3238-3435  $\nu$ (N-H), 1671  $\nu$ (C=O), 1206  $\nu$ (C=S); <sup>1</sup>H NMR (400 MHz,  
217 CDCl<sub>3</sub>, ppm): 13.48 (s, 1H, NH), 11.55 (s, 1H, NH), 8.27 (d, 4H, *J* = 8 Hz), 7.75 (d, 2H, *J* = 8  
218 Hz), 7.53 (t, 1H, *J* = 8 Hz), 7.41 (t, 2H, *J* = 8 Hz), 1.59 (s, 15H); ESI-MS (m/z): 538.08[M-2Cl]<sup>+</sup>;  
219 UV-Vis {Acetonitrile,  $\lambda_{\max}$  nm ( $\epsilon/10^{-4}$  M<sup>-1</sup> cm<sup>-1</sup>): 259 (1.71). Anal. Calc. for C<sub>24</sub>H<sub>26</sub>Cl<sub>2</sub>N<sub>3</sub>O<sub>3</sub>RhS  
220 (610.36): C, 47.23; H, 4.29; N, 6.88. Found: C, 47.25; H, 4.30; N, 6.74.

221 2.6.9. [Cp\*Ir( $\kappa^1$ <sub>(S)</sub>-L3)Cl<sub>2</sub>] (9)

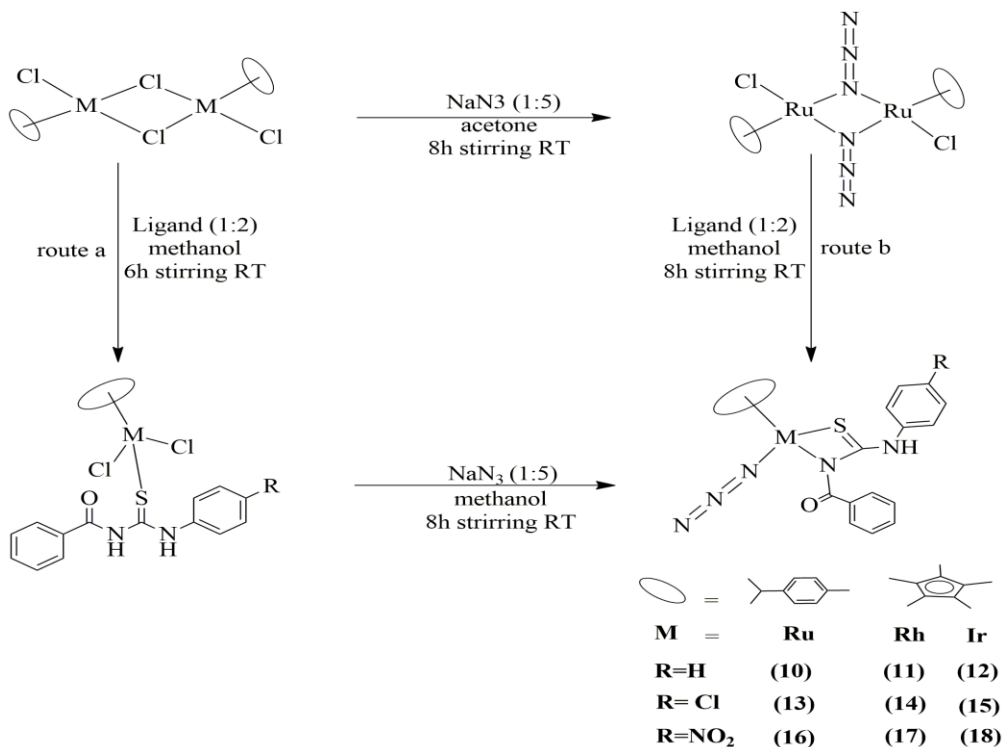
222 Yield: (79%) ;IR (KBr, cm<sup>-1</sup>): 3241-3447  $\nu$ (N-H), 1671  $\nu$ (C=O), 1210  $\nu$ (C=S); <sup>1</sup>H NMR (400 MHz,  
223 CDCl<sub>3</sub>, ppm) : 13.53 (s, 1H, NH), 12.03 (s, 1H, NH), 8.42 (d, 2H, *J* = 4 Hz), 8.34 (d, 2H, *J* = 8  
224 Hz), 7.80 (d, 2H, *J* = 4 Hz), 7.63 (t, 1H, *J* = 8 Hz), 7.55 (t, 2H, *J* = 8 Hz), 1.64 (s, 15H); ESI-MS  
225 (m/z): 626.14 [M-2Cl]<sup>+</sup>; UV-Vis {Acetonitrile,  $\lambda_{\max}$  nm ( $\epsilon/10^{-4}$  M<sup>-1</sup> cm<sup>-1</sup>): 275 (1.11), 345  
226 (0.22). Anal. Calc. for C<sub>24</sub>H<sub>26</sub>Cl<sub>2</sub>IrN<sub>3</sub>O<sub>3</sub>S (699.67): C, 41.20; H, 3.75; N, 6.01. Found: C, 41.19;  
227 H, 3.78; N, 6.17.

228 2.7. General procedure for synthesis of azido complexes (10-18)

229 For the synthesis of azido complexes **10-18** these two reaction routes are possible:-

230 Route a: A suspension of the corresponding starting complexes **1-9** and NaN<sub>3</sub> in 1:5 molar ratios  
 231 was suspended in dry methanol (10 ml) and stirred at room temperature for 8h (Scheme 3). The  
 232 solvent was removed to dryness using rotary evaporator. The residue was extracted with  
 233 dichloromethane, filtered and precipitated with hexane. This accounts for the higher yield of  
 234 complexes by this route as compared to that obtained by the other route (route b).

235 Route b: In addition, the terminal azido complexes **10, 13, 16** have also been prepared by  
 236 treatment of azido dimer [(p-cymene)Ru(μ-N<sub>3</sub>)Cl]<sub>2</sub> with Ligands **L1-L3** in dry methanol. The  
 237 resulting mixture was stirred for 8h at room temperature. After completion of the reaction, the  
 238 solvent was removed to dryness using rotary evaporator the expected complex was extracted  
 239 with dichloromethane, filtered, precipitated with hexane and dried in vacuum.



240

241 **Scheme 3.** Schematic representation for the synthesis of complexes (**10-18**)

242 2.7.1. [(*p*-cymene)Ru( $\kappa^2_{(N,S)}$ -L1)N<sub>3</sub>] (**10**)

243 Yield: (68%); IR (KBr, cm<sup>-1</sup>): 3433  $\nu_{(N-H)}$ , 2030  $\nu_{(N_3)}$ , 1617  $\nu_{(C=O)}$ , 1192  $\nu_{(C=S)}$ ; <sup>1</sup>H NMR (400  
244 MHz, CDCl<sub>3</sub>, ppm): 12.54 (s, 1H), 8.04 (d, 2H, J = 8 Hz), 7.51-7.58 (m, 5H), 7.40 (t, 2H, J = 8  
245 Hz), 7.28 (d, 1H, J = 8 Hz), 5.24 (d, 1H, J = 4 Hz), 4.67 (d, 1H, J = 4 Hz), 4.62 (d, 1H, J = 4 Hz),  
246 4.46 (d, 1H, J = 8 Hz), 2.60-2.70 (sept, 1H), 2.09 (s, 3H), 1.20 (d, 6H, J = 8 Hz). <sup>13</sup>C NMR (100  
247 MHz, CDCl<sub>3</sub>, ppm): 186.06, 178.67, 137.58, 135.40, 131.14, 129.20, 128.07, 123.82, 100.86,  
248 100.28, 83.90, 83.11, 80.40, 78.57, 31.27, 23.26, 21.76, 18.02; UV-Vis {Acetonitrile,  $\lambda_{max}$  nm  
249 ( $\epsilon/10^{-4}$  M<sup>-1</sup> cm<sup>-1</sup>): 284 (0.75), 422 (0.18).

250 2.7.2. [Cp\*Rh( $\kappa^2_{(N,S)}$ -L1)N<sub>3</sub>] (**11**)

251 Yield: (68%); IR (KBr, cm<sup>-1</sup>): 3436  $\nu_{(N-H)}$ , 2034  $\nu_{(N_3)}$ , 1627  $\nu_{(C=O)}$ , 1191  $\nu_{(C=S)}$ ; <sup>1</sup>H NMR (400 MHz,  
252 CDCl<sub>3</sub>, ppm): 12.74 (s, 1H), 8.21 (d, 2H, J = 8 Hz), 7.55 (t, 3H, J = 8 Hz), 7.47-7.52 (m, 3H),  
253 7.40 (t, 3H, J = 8 Hz), 1.41 (s, 15H); ESI-MS (m/z): 493.16 [M-N<sub>3</sub>]<sup>+</sup>. UV-Vis {Acetonitrile,  $\lambda_{max}$   
254 nm ( $\epsilon/10^{-4}$  M<sup>-1</sup> cm<sup>-1</sup>): 293 (0.85), 422 (0.18). Anal. Calc. for C<sub>24</sub>H<sub>26</sub>N<sub>5</sub>ORhS (535.97): C, 53.83;  
255 H, 4.89; N, 13.08. Found: C, 53.87; H, 4.82; N, 13.11.

256 2.7.3. [Cp\*Ir( $\kappa^2_{(N,S)}$ -L1)N<sub>3</sub>] (**12**)

257 Yield: (56%); IR (KBr, cm<sup>-1</sup>): 3420  $\nu_{(N-H)}$ , 2036  $\nu_{(N_3)}$ , 1618  $\nu_{(C=O)}$ , 1198  $\nu_{(C=S)}$ ; <sup>1</sup>H NMR (400  
258 MHz, CDCl<sub>3</sub>, ppm): 12.75 (s, 1H), 8.22 (d, 1H, J = 8 Hz), 8.10 (d, 1H, J = 8 Hz), 7.57 (d, 1H, J =  
259 8 Hz), 7.48 (t, 3H, J = 4 Hz), 7.40 (d, 2H, J = 4 Hz), 7.33 (d, 1H, J = 4 Hz), 1.65 (s, 15H). <sup>13</sup>C  
260 NMR (100 MHz, CDCl<sub>3</sub>, ppm): 173.44, 167.77, 145.68, 139.88, 130.33, 129.59, 127.42, 125.25,  
261 126.25, 89.45, 9.02; ESI-MS (m/z): 582.80 [M-N<sub>3</sub>]<sup>+</sup>. UV-Vis {Acetonitrile,  $\lambda_{max}$  nm ( $\epsilon/10^{-4}$  M<sup>-1</sup>  
262 cm<sup>-1</sup>): 204 (0.832), 361 (0.41).

263 2.7.4. [(*p*-cymene)Ru( $\kappa^2_{(N,S)}$ -L2)N<sub>3</sub>] (**13**)

264 Yield: (71%); IR (KBr, cm<sup>-1</sup>): 3433  $\nu_{(N-H)}$ , 2030  $\nu_{(N_3)}$ , 1611  $\nu_{(C=O)}$ , 1193  $\nu_{(C=S)}$ ; <sup>1</sup>H NMR (400  
265 MHz, CDCl<sub>3</sub>, ppm): 12.50 (s, 1H), 8.02 (d, 2H, J = 4 Hz), 7.51-7.58 (m, 3H), 7.46 (d, 2H, J = 8  
266 Hz), 7.35 (d, 2H, J = 12 Hz), 5.25 (d, 1H, J = 8 Hz), 4.67 (d, 1H, J = 4 Hz), 4.62 (d, 1H, J = 4

267 Hz), 4.46 (d, 1H, J = 4 Hz), 2.59-2.69 (sept, 1H), 2.08 (s,3H), 1.19 (d, 6H); <sup>13</sup>C NMR (100  
268 MHz,CDCl<sub>3</sub>, ppm): 189.13, 178.67, 131.97, 129.33, 129.02, 128.79, 128.08, 127.18, 125.17,  
269 121.57, 99.67, 97.27, 83.82, 81.96, 80.10, 31.28, 30.18, 22.31, 17.52; UV-Vis {Acetonitrile, λ<sub>max</sub>  
270 nm (ε/10<sup>-4</sup> M<sup>-1</sup> cm<sup>-1</sup>): 277 (0.92), 443 (0.16).

271 2.7.5. [Cp\*Rh(κ<sup>2</sup><sub>(N,S)</sub>-L2)N<sub>3</sub>] (**14**)

272 Yield: (65%); IR (KBr, cm<sup>-1</sup>): 3423 ν<sub>(N-H)</sub>, 2037 ν<sub>(N<sub>3</sub>)</sub>, 1621 ν<sub>(C=O)</sub>, 1190 ν<sub>(C=S)</sub>; <sup>1</sup>H NMR (400  
273 MHz, CDCl<sub>3</sub>, ppm): 12.72 (s,1H), 8.20 (d, 2H, J = 8 Hz), 7.49-7.52 (m, 5H), 7.35 (d, 2H, J = 12  
274 Hz), 1.41 (s, 15H); <sup>13</sup>C NMR (100 MHz,CDCl<sub>3</sub>, ppm): 186.76, 176.69, 134.59, 134.35, 131.92,  
275 131.66, 129.28, 128.94, 127.61, 127.18, 93.15, 8.72; UV-Vis {Acetonitrile, λ<sub>max</sub> nm (ε/10<sup>-4</sup> M<sup>-1</sup>  
276 cm<sup>-1</sup>): 265 (0.90), 430 (0.17)}. Anal. Calc. for C<sub>24</sub>H<sub>25</sub>ClN<sub>3</sub>ORhS (569.91): C, 50.58; H, 4.42; N,  
277 12.29. Found: C, 50.65; H, 4.45; N, 12.18.

278 2.7.6. [Cp\*Ir(κ<sup>2</sup><sub>(N,S)</sub>-L3)N<sub>3</sub>] (**15**)

279 Yield: (54%); IR (KBr, cm<sup>-1</sup>): 3402 ν<sub>(N-H)</sub>, 2037 ν<sub>(N<sub>3</sub>)</sub>, 1619 ν<sub>(C=O)</sub>, 1194ν<sub>(C=S)</sub>; <sup>1</sup>H NMR (400  
280 MHz, CDCl<sub>3</sub>, ppm): 8.04 (d, 2H, J = 8 Hz), 7.47 (d, 2H, J = 8 Hz), 7.37 (t, 3H, J = 8 Hz), 6.59 (d,  
281 2H, J = 12 Hz), 1.68 (s, 15H); ESI-MS (m/z): 612.96 [M-N<sub>3</sub>]<sup>+</sup>.UV-Vis {Acetonitrile, λ<sub>max</sub> nm  
282 (ε/10<sup>-4</sup> M<sup>-1</sup> cm<sup>-1</sup>): 257 (0.59), 361(0.22).

283 2.7.7. [(p-cymene)Ru(κ<sup>2</sup><sub>(N,S)</sub>-L3)N<sub>3</sub>] (**16**)

284 Yield: (69%); IR (KBr, cm<sup>-1</sup>): 3432 ν<sub>(N-H)</sub>, 2035 ν<sub>(N<sub>3</sub>)</sub>, 1627 ν<sub>(C=O)</sub>, 1189 ν<sub>(C=S)</sub>; <sup>1</sup>H NMR (400  
285 MHz, CDCl<sub>3</sub>, ppm):12.98 (s, 1H), 8.26 (d, 2H, J = 8 Hz), 8.03 (d, 2H, J = 8 Hz), 7.76 (d, 2H, J =  
286 8 Hz), 7.53- 7.62 (m, 3H), 5.30 (d, 1H, J = 8 Hz), 4.72 (d, 1H, J = 8 Hz), 4.66 (d, 1H, J = 8 Hz),  
287 4.50 (d, 1H, J = 4 Hz), 2.61-2.71 (sept, 1H), 2.10 (s, 3H), 1.21 (d, 6H, J = 8 Hz); ESI-MS (m/z):  
288 536.08 [M-N<sub>3</sub>]<sup>+</sup>. UV-Vis {Acetonitrile, λ<sub>max</sub> nm (ε/10<sup>-4</sup> M<sup>-1</sup> cm<sup>-1</sup>): 278(1.16), 339 (0.68)}. Anal.

289 Calc. for C<sub>24</sub>H<sub>24</sub>N<sub>6</sub>O<sub>3</sub>RuS (577.62): C, 49.90; H, 4.19; N, 14.55. Found: C, 49.89; H, 4.23; N,  
290 14.68.

291 2.7.8. [Cp\*Rh( $\kappa^2_{(N,S)}-L3$ )N<sub>3</sub>] (**17**)

292 Yield: (58%); IR (KBr, cm<sup>-1</sup>): 3428  $\nu_{(N-H)}$ , 2034  $\nu_{(N_3)}$ , 1614  $\nu_{(C=O)}$ , 1193  $\nu_{(C=S)}$ ; <sup>1</sup>H NMR (400  
293 MHz, CDCl<sub>3</sub>, ppm): 13.13 (s, 1H), 8.20 (d, 2H, J = 8 Hz), 8.13 (d, 2H, J = 8 Hz), 7.73 (d, 2H, J  
294 = 8 Hz), 7.49 (t, 1H, J = 8 Hz), 7.43 (t, 1H, J = 8 Hz), 1.36 (s, 15H); ESI-MS (m/z): 537.08 [M-  
295 N<sub>3</sub>]<sup>+</sup>. UV-Vis {Acetonitrile,  $\lambda_{max}$  nm ( $\epsilon/10^{-4}$  M<sup>-1</sup> cm<sup>-1</sup>)}: 269 (0.96), 338 (0.68), 432 (0.16).

296 2.7.9. [Cp\*Rh( $\kappa^2_{(N,S)}-L3$ )N<sub>3</sub>] (**18**)

297 Yield: (62%); IR (KBr, cm<sup>-1</sup>): 3432  $\nu_{(N-H)}$ , 2030  $\nu_{(N_3)}$ , 1627  $\nu_{(C=O)}$ , 1202  $\nu_{(C=S)}$ ; <sup>1</sup>H NMR (400  
298 MHz, CDCl<sub>3</sub>, ppm): 8.39 (d, 1H, J = 8 Hz), 7.96 (d, 1H, J = 8 Hz), 7.83 (d, 1H, J = 8 Hz), 7.71  
299 (d, 2H, J = 8 Hz), 7.50 (d, 2H, J = 8 Hz), 7.37 (t, 2H, J = 8 Hz), 1.74 (s, 15H); ESI-MS (m/z):  
300 628.14 [M-N<sub>3</sub>]<sup>+</sup>. UV-Vis {Acetonitrile,  $\lambda_{max}$  nm ( $\epsilon/10^{-4}$  M<sup>-1</sup> cm<sup>-1</sup>)}: 281 (0.44), 344 (0.30).

### 301 3. Results and discussion

#### 302 3.1. Synthesis of complexes

303 The metal complexes **1-9** were synthesized by the reaction of Ru, Rh and Ir metal  
304 precursors with the thiourea ligands **L1-L3** in methanol and are represented in (Scheme 2). All  
305 these metal complexes were obtained in good yield and are yellow or red in color. They are  
306 stable in air as well as in solid state, and are non-hygroscopic. These complexes were isolated as  
307 neutral complexes with mono-dentate  $\kappa^1_{(S)}$  coordination. Azido compounds were synthesized by  
308 the substitution of the chloride ligand by azide group following two routes. Treatment of half-  
309 sandwich mononuclear complexes **1-9** with five fold of NaN<sub>3</sub> in methanol (Scheme 3) resulted in  
310 the substitution of the chloride ligand and the formation of highly strained four membered  
311 chelated  $\kappa^2_{(N,S)}$  azido complexes **10-18** (Scheme 3 route a). Similarly, these terminal azido

312 complexes **10**, **13**, and **16** can be prepared from the binuclear *p*-cymene ruthenium azido  
313 complexes [(*p*-cymene)Ru( $\mu$ -N<sub>3</sub>)Cl]<sub>2</sub> by reacting with ligand L1-L3 in methanol (route b).  
314 However, ‘route a’ is more preferable than ‘route b’ as it gives higher percentage yield of the  
315 expected complex, hence we reported the yield obtained through this route in the experimental  
316 section. Our effort to make triazole complexes by reaction of terminal azido complexes with  
317 excess of dimethylacetylenedicarboxylate (MeO<sub>2</sub>CC<sub>2</sub>CO<sub>2</sub>Me) or diethylacetylenedicarboxylate  
318 (EtO<sub>2</sub>CC<sub>2</sub>CO<sub>2</sub>Et) in dichloromethane was unsuccessful. Further we have carried out the  
319 antibacterial studies for ligands and complexes against four pathogenic bacteria *viz.*, *S. aureus*, *E.*  
320 *coli*, *B. thuringiensis* and *P. aeruginosa* but none of the compounds showed any activity. All the  
321 synthesized complexes are soluble in common organic solvents such as dichloromethane,  
322 acetonitrile and acetone but insoluble in diethyl ether and hexane. All the synthesized ligands  
323 and complexes were fully characterized by various spectroscopic techniques.

### 324 3.2. Spectroscopic characterization of Complexes

325 The IR spectra of free aroyl thiourea ligands showed characteristic stretching frequencies  
326 at 3076-3312 cm<sup>-1</sup> corresponding to  $\nu_{(N-H)}$  which also present in the same region in all the  
327 complexes indicating that deprotonation does not occur. A strong band observed in the region  
328 1657–1661 cm<sup>-1</sup> in the FT-IR spectra of the ligands was assigned to the  $\nu_{(C=O)}$ , the stretching  
329 vibration  $\nu_{(C=O)}$  bands remain unaltered upon complexation indicating non participation of  
330 carbonyl oxygen in coordination. The characteristic band for  $\nu_{(C=S)}$  appeared at 1232–1241 cm<sup>-1</sup>  
331 in the spectra of L1-L3 was shifted to lower frequency (1189–1213 cm<sup>-1</sup>) on complexation  
332 indicating involvement of sulfur in coordination to the metal center.

333 The IR spectra of the azido complexes **10-18** showed sharp absorption band at  
334 frequencies 2030-2037 cm<sup>-1</sup> corresponding to terminal  $\nu_{N_3}$ . When synthesis *via* route b the IR

335 spectra of these complexes also show absence of the bridging azido band at  $2065\text{ cm}^{-1}$  and the  
336 appearance of new bands for terminal azido group in the above mentioned range. This leads us to  
337 infer the formation of terminal azido complexes.

338 The  $^1\text{H}$  NMR spectra of the complexes **1-9** (Figure S1-S8) show a downfield shift in  
339 protons of ligand after forming complexes, which is due to the deshielding effect exerted by  
340 metal on the ligands. The  $^1\text{H}$  NMR of the complexes **1-9** show two singlet around 13.53-12.96  
341 and 11.88-11.29 which is attributed to the N-H proton signals of thiocarbonyl and carbonyl  
342 attached N-H respectively. The appearance of two N-H signals in all the complexes indicates that  
343 the N-H group is not involved in bonding. Resonances due to the aromatic ligands protons were  
344 all in the expected range of 8.29-7.21 ppm, which indicates the coordination of the thiourea  
345 ligand to the metal center. In addition to the signals for the ligand protons, a sharp singlet was  
346 observed for all the rhodium and iridium complexes between 1.58-1.63 ppm corresponding to the  
347 methyl protons of the Cp\* ring. The  $^1\text{H}$  NMR spectra of complexes **1**, **4** and **7** displays a doublet  
348 for methyl protons of isopropyl group at 1.23 ppm, 1.30 ppm and 1.31 ppm respectively, a  
349 singlet at 2.17 ppm, 2.24 ppm and 2.27 ppm for methyl group, a septet at 2.86 ppm, 2.94 ppm  
350 and 2.96 ppm for one proton of isopropyl group of *p*-cymene moiety. Two doublets were  
351 observed in the range 5.18 ppm- 5.45 ppm corresponds to the aromatic protons of *p*-cymene.

352 The  $^1\text{H}$  NMR spectra of all the azido complexes **10-18** (Figure S9-S16) show the  
353 disappearance of one N-H proton, which strongly supports the deprotonation of one amido  
354 hydrogen and this has also been confirmed from molecular structures. The deprotonation of  
355 amido hydrogen (NH) resulted in the generation of negative charge on amido nitrogen atom,  
356 which leads to the formation of neutral complexes **10-18**. The azido complexes show a singlet  
357 around 12.50-13.13, which is attributed to one N-H proton signals. The appearance of one N-H

358 signal in all the complexes indicates that only one N-H group involved in bonding. Resonances  
359 due to the aromatic ligands protons were all in the same range of 8.40-7.27 ppm. The rhodium  
360 and iridium complexes displayed only one singlet for the methyl protons of the Cp\* group  
361 around 1.52-1.75 ppm. The binding of the azide ligand to the ruthenium atom in mononuclear  
362 ruthenium complexes leads to the splitting of the *p*-cymene ring protons upon coordination of the  
363 ligand to the *p*-cymene moiety. The signals associated with the *p*-cymene ring protons consisted  
364 of four doublets around 5.29-4.50 ppm. This unexpected pattern of signals for the *p*-cymene  
365 ligand is consisted with the metal center being chiral upon coordination of the azide ligand and  
366 these results correlates well with similar reported complexes [35]. In addition the methine and  
367 methyl protons of the *p*-cymene group exhibited septet around 2.65 ppm and singlet around 2.09  
368 ppm.

369 The <sup>13</sup>C NMR spectra of the complexes further justify the coordination of the ligands and  
370 formation of complexes. The <sup>13</sup>C NMR spectra of the representative complexes are provided in  
371 the supplementary information (Figures S29-S31). The <sup>13</sup>C NMR spectra of the complexes  
372 displayed signals associated with the ligand carbons, *p*-cymene ligand carbons, methyl carbon of  
373 Cp\* and ring carbon of Cp\*. The carbon resonance of the thiocarbonyl (C=S) group appeared in  
374 the lower frequency region around 173.44 to 186.76 ppm and the carbonyl (C=O) group  
375 appeared in the range of 178.67 to 167.77 ppm. The aromatic carbons signals for the ligands  
376 were observed in the range of 121.57 to 145.68 ppm. The methyl, methine and isopropyl carbon  
377 resonances of the *p*-cymene ligand were observed in the region around 17.52 to 31.28 ppm. The  
378 signals associated with the ring carbons of the Cp\* ligand was observed in the region 89.45 to  
379 93.15 ppm in contrast the methyl carbon resonances was observed as a sharp peak at 8.72 and

380 9.02 ppm. Overall results from the NMR spectral studies strongly support the formation of the  
381 metal complexes.

382 The mass spectra of the complexes are presented in the supplementary information Figure  
383 S17-S28. Complexes display their predominant molecular ion peaks at m/z: 490.96, 493.02,  
384 581.01, 524.23, 527.19, 617.22, 535.13, 538.08 and 659.12 respectively which correspond to [M-  
385 2Cl]<sup>+</sup> ion peak. Complexes 11, 12, 15, 16, 17, and 18 display their predominant peaks at m/z:  
386 493.16, 582.80, 616.96, 536.08, 537.08, and 628.14 respectively which correspond to [M-N<sub>3</sub>]<sup>+</sup>.  
387 The appearance of these peaks in its mass spectra clearly indicates the formation of thiourea  
388 metal complexes. The peaks corresponding to the loss of the thiourea ligands as well as the arene  
389 ring are not observed which indicates the strong metal to ligand and metal to arene bond. The  
390 mass spectral values strongly justify the composition and formation of these complexes.

391 The electronic spectra of the complexes were recorded in acetonitrile at 10<sup>-4</sup> M  
392 concentration at room temperature. The electronic spectra of complexes display two absorption  
393 band in the higher energy region around 230-340 nm (figure S32-33). The band in the range of  
394 230-280 nm can be assigned as  $\pi$ - $\pi^*$  and n- $\pi^*$  transition. The band in the lower energy region  
395 around 345-405 nm can be assigned as metal (d $\pi$ ) to  $\pi^*$  ligand charge transfer (MLCT).

### 396 3.3. Description of the molecular structures of complexes

397 The molecular structure of the complexes along with the crystallographic numbering  
398 schemes is depicted in the Figures 1-7. Because of low theta value the crystal structures of  
399 complexes **6** and **17** are presented here to only confirm the structure and composition of  
400 molecule. The summary of the crystal data, data collection and structure refinement parameters  
401 are summarized in Table S1 and Table S2. Selected bond lengths, bond angles and metal atom  
402 involving ring centroid values are listed in Table 1 and Table 2. The crystals of the complexes **2**,

403 **3, 4, 5, 6, 7, 8, 10, 16** and **17** suitable for X-ray diffraction study were obtained by slow diffusion  
404 of hexane to the concentrated dichloromethane solutions of the compound. By carrying out the  
405 single crystal analyses we were able to confirm the variety of bonding modes associated with the  
406 ligand. The complexes adopted a piano-stool geometry, where *p*-cymene and Cp\* moiety served  
407 as the top of the stool and the three leg sites were occupied by sulfur from ligands and two  
408 terminal chlorides. The metal atom in these complexes is situated in a pseudo-octahedral  
409 arrangement with the ligand coordinating through the sulfur atom. In complexes **1-9** the thiourea  
410 ligands acted as a neutral mono-dentate ligand coordinating metal *via* S atom.

411       Complexes **2, 3, 5** and **8** crystallized in monoclinic with space group *P2<sub>1</sub>/c*. Complex **4**  
412 crystallized in monoclinic system with space group *C2/c*, whereas Complex **7** crystallized in  
413 triclinic system with space group *PT*. The distance between the metal M to centroid of the *p*-  
414 cymene/Cp\* ring are {1.787 (**2**), 1.778 (**3**), 1.672 (**4**), 1.689 (**5**), 1.665 (**7**), 1.784 (**8**) Å}. The  
415 metal to sulfur bond distances of complexes **2, 3, 4, 5, 7** and **8** were found to be 2.395(1),  
416 2.370(2), 2.418(1), 2.366(1), 2.4004(7) and 2.3857 (8) respectively, whereas the M-Cl1 bond  
417 distances of complexes **2, 3, 4, 5, 7** and **8** were found to be 2.413(1), 2.423(1), 2.426(1),  
418 2.440(1), 2.4338(5) and 2.4253(9) and the M-Cl2 bond distances were found to be 2.427(1),  
419 2.410 (2), 2.406 (1), 2.425 (1), 2.4319 (7) and 2.411 (1) respectively which are comparable with  
420 earlier reported complexes [34]. The C-S bond length in these complexes lie in the range 1.688-  
421 1.703 Å which are in good agreement with other related compounds for a C=S double bond [40].  
422 The bond angle values S-M-Cl and Cl-M-Cl are found to be in the range 87.67-94.09° thus  
423 suggesting the pseudo octahedral arrangement around the metal center.

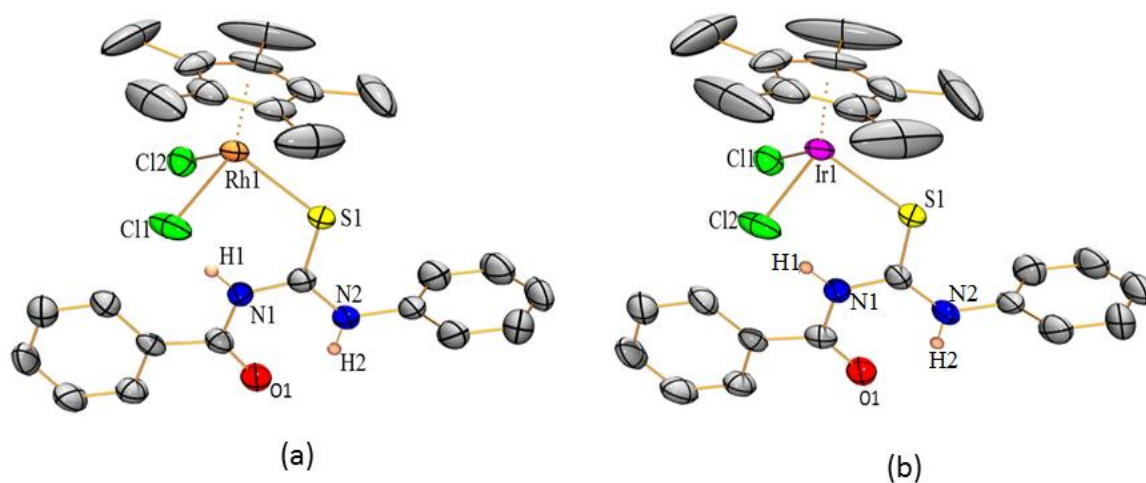
424       Further reaction of the mono-dentate thiourea *p*-cymene ruthenium, Cp\* rhodium and  
425 Cp\* iridium complexes with excess of sodium azide resulted in deprotonation of the amido

426 hydrogen which changed the bonding behavior of the thiourea ligand towards both *p*-cymene  
427 ruthenium and Cp\* rhodium complexes as confirmed from the molecular structures. X-ray  
428 studies of these complexes revealed that upon coordination of azide group to the metal it cause  
429 deprotonation of amido N-H and the bonding of the thiourea derivatives were altered. All the  
430 thiourea derivatives revealed interesting coordination towards metal upon coordination of the  
431 azide group. The *p*-cymene ruthenium azido complexes **10** and **16** crystallized in monoclinic  
432 system with space group *P 21/c* and *P21/n* respectively. Whereas the Cp\*rhodium azido complex  
433 **17** crystallized in monoclinic system with space group *P2<sub>1</sub>/n*. The deprotonation of the amido  
434 hydrogen (NH) forced the thiourea ligand to coordinate metal in an anionic bidentate chelating  
435 fashion via S and N thus forming a highly strained four membered chelated ring and the  
436 oxidation state of metal is balanced by the amido group nitrogen and azide nitrogen. The distance  
437 between the metal M to centroid of the *p*-cymene/Cp\* ring in complexes **10**, **16** and **17** are 1.675,  
438 1.678 and 1.784 Å [41]. The metal to sulfur bond distance of complex **16** is 2.406(1) was found  
439 to be slightly longer than complex **17** 2.398(2) Å whereas the metal to azide bond distance are  
440 2.107(4) and 2.125(5) Å respectively. The C=S bond length in complex **17** is 1.723(4) Å was  
441 slightly longer than that in complex **16** 1.711(4) Å. The bond angle values N-M-N and N-M-S  
442 for complexes **10**, **16** and **17** are given in Table 2. The bite angle of complexes **10**, **16** and **17** are  
443 67.27°, 65.86° and 67° respectively which is the strain angle giving a pseudo-octahedral  
444 arrangement of piano stool half sandwich complex.

445 Furthermore, the crystal structure of complex **3** display two different types of interaction  
446 intramolecular and intermolecular hydrogen bonding; the first interaction is N-H...O between the  
447 carbonyl oxygen and amido H-atom (1.907 Å), and the N-H...Cl between the other amido  
448 hydrogen and Cl-atom attached to iridium metal (2.424 Å). The second is C-H... $\pi$  interaction

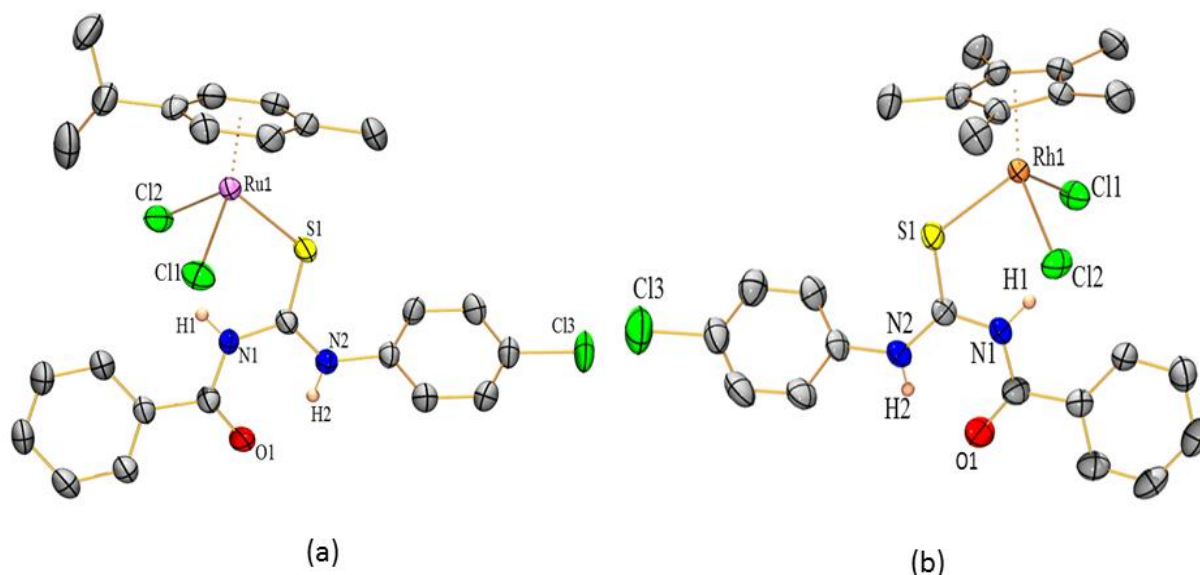
449 between the benzoyl moiety and the H-atom of aniline (3.517 Å) (Figure S34). Similarly the  
450 crystal structure of complex **16** exhibits N-H...O interaction between the carbonyl oxygen and  
451 amido H-atom (1.902Å), the C-H...N interaction between the H-atom of *p*-cymene and azide  
452 nitrogen (2.758 Å), and C-H...O interaction between the H-atom of *p*-cymene and O-atom of  
453 nitro group (2.415 Å) (Figure S35).

454

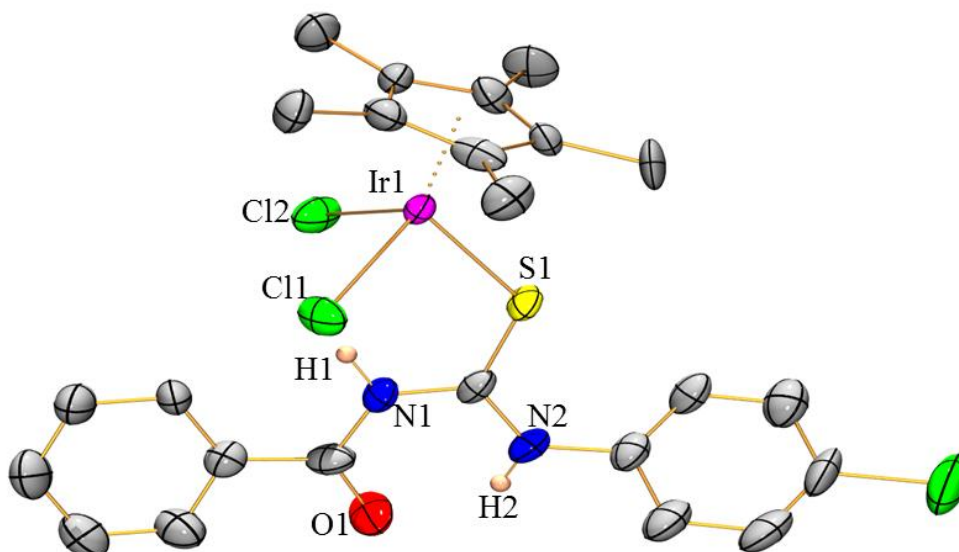


455  
456 **Figure 1.** (a) ORTEP diagram of complex **2** and (b) ORTEP diagram of complex **3** with 50%  
457 probability thermal ellipsoids. Hydrogen atoms (except on N) are omitted for clarity.

458

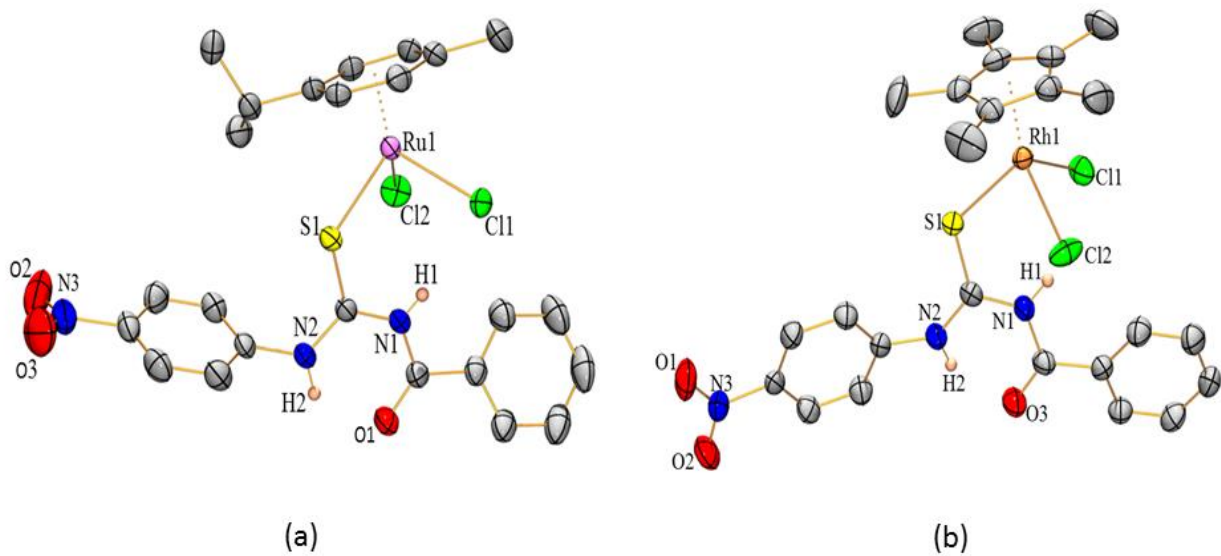


459  
 460 **Figure 2.** (a) ORTEP diagram of complex **4** and (b) ORTEP diagram of complex **5** with 50%  
 461 probability thermal ellipsoids. Hydrogen atoms (except on N) are omitted for clarity.

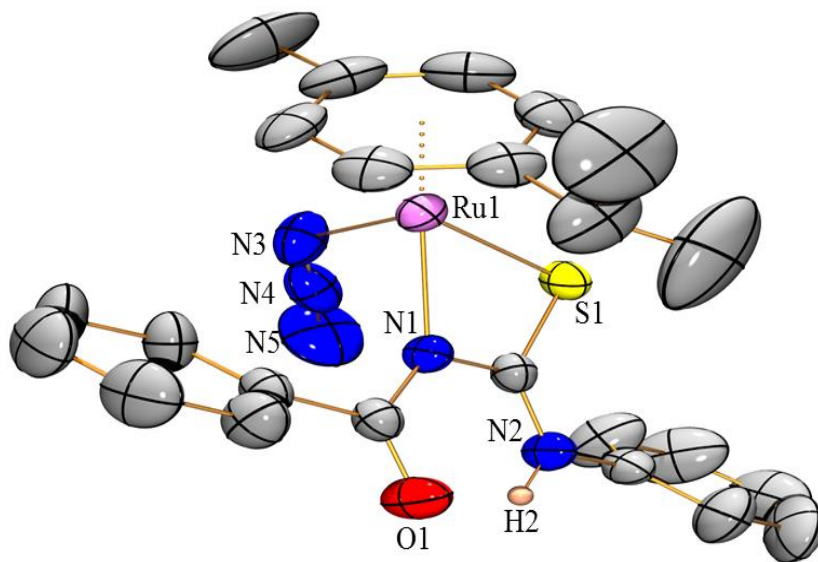


462  
 463 **Figure 3.** ORTEP diagram of complex **6** with 50% probability thermal ellipsoids. Hydrogen  
 464 atoms (except on N) are omitted for clarity. Because of low theta value the crystal structure of  
 465 complex are presented here to only confirm the structure and composition of molecule.

466

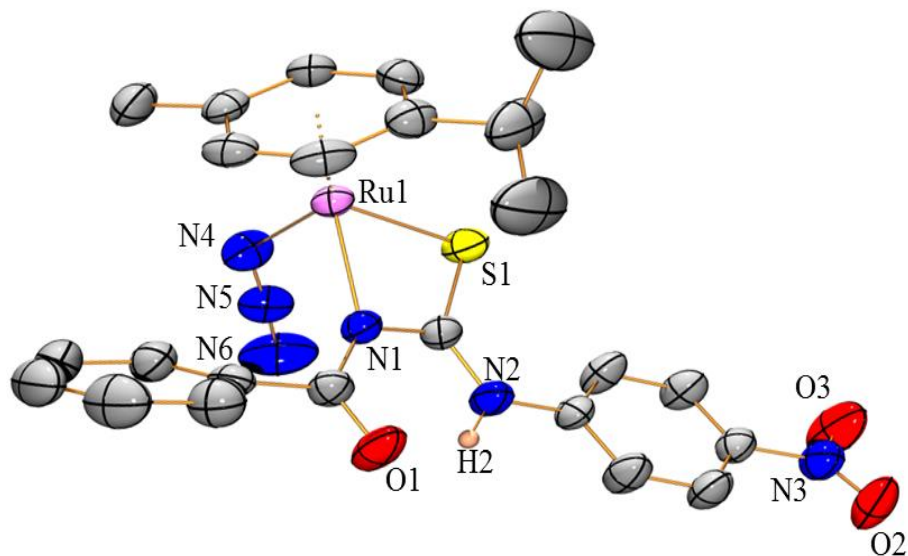


467  
 468 **Figure 4.** (a) ORTEP diagram of complex **7** and (b) ORTEP diagram of complex **8** with 50%  
 469 probability thermal ellipsoids. Hydrogen atoms (except on N) are omitted for clarity.



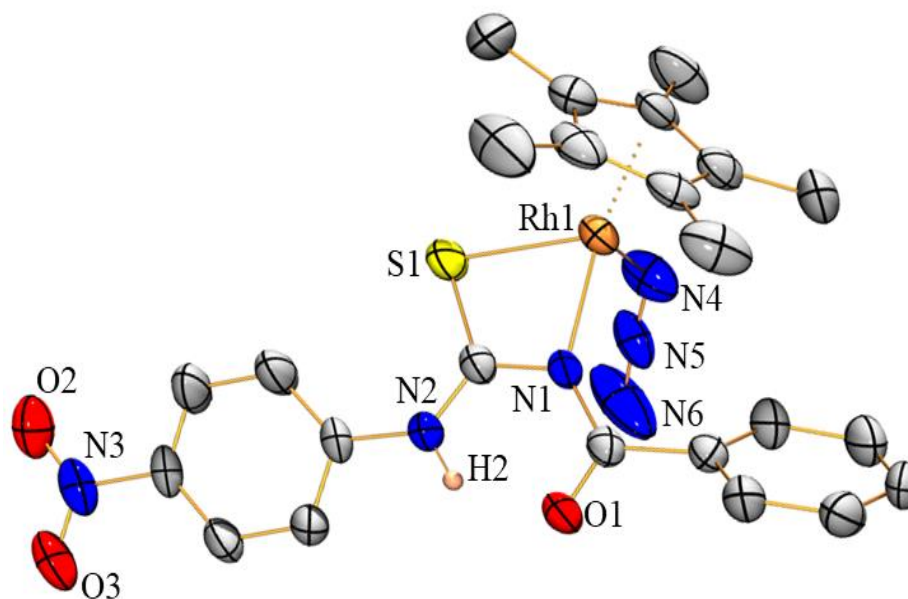
470  
 471 **Figure 5.** ORTEP diagram of complex **10** with 50% probability thermal ellipsoids. Hydrogen  
 472 atoms (except on N) are omitted for clarity.

473



474

475 **Figure 6.** ORTEP diagram of complex **16** with 50% probability thermal ellipsoids. Hydrogen  
 476 atoms (except on N) are omitted for clarity.



477

478 **Figure 7.** ORTEP diagram of complex **17** with 50% probability thermal ellipsoids. Hydrogen  
 479 atoms (except on N) are omitted for clarity. Because of low theta value the crystal structure of  
 480 complex are presented here to only confirm the structure and composition of molecule.

481

### 482 3.5. Chemosensitivity studies

483 The complexes (**1-9**) were tested for their cytotoxicity against cancer cell line HCT-116  
484 (human colon carcinoma) and non-cancer cell line ARPE-19 (human retinal epithelial cells). The  
485 response of the cell lines HCT-116 and ARPE-19 (human retinal epithelial cells) to the test  
486 complexes **1-9** and cisplatin is presented in tabular form in [Table 3](#). Complexes **5**, **6**, and **8** were  
487 found to be inactive against both the cell line with  $IC_{50}$  values  $> 100 \mu\text{M}$ . Complexes **1**, **2**, **7** and  
488 **9** were found to be less active against HCT-116 cell line. In contrast complexes **3** and **4**  
489 displayed moderate activity against both cell lines with  $IC_{50}$  value of  $35.172 \pm 1.175$  and  $43.751$   
490  $\pm 2.480 \mu\text{M}$ . Of the complexes evaluated complex **3** was the most potent against both cell lines.  
491 The selectivity index (SI) is shown in [Table 3](#), which is defined as the ratio of  $IC_{50}$  values in  
492 ARPE-19 cells divided by the  $IC_{50}$  of HCT-116 cells. Complex **3** was also the most selective of  
493 the novel complexes evaluated with equitoxic activity observed against both HCT-116 and  
494 ARPE-19 cells. Whilst these complexes were not as potent as cisplatin, complex **3** has a  
495 selectivity index that is comparable to cisplatin (SI=1.078 and 1.233 respectively) and it is  
496 therefore the most promising complex in this series.

497  $IC_{50}$  = concentration of the drug required to inhibit the growth of 50% of the cancer cells ( $\mu\text{M}$ ).

### 498 4. Conclusion

499 In this work, we have successfully synthesized  $d^6$  half-sandwich metal complexes bearing  
500 thiourea ligands and the reactivity of these complexes towards  $\text{NaN}_3$ . The ligands used in this  
501 work exhibited interesting binding modes on reacting with sodium azide. Further reactions of  
502 mono-dentate complexes **1-9** with  $\text{NaN}_3$  resulted in deprotonation of amido hydrogen and  
503 change the coordination mode of the thiourea derivative from mono-dentate to bidentate  
504 chelating mode. This complexes **10-18** coordinate in a highly strained four membered chelated

505  $\kappa^2_{(N,S)}$  towards the metal atoms rather than the six membered chelated  $\kappa^2_{(O,S)}$ . As there are two  
506 amido groups in the thiourea derivative we expect the coordination of the other amido group as  
507 well, but the molecular structure revealed that only the amido adjacent to carbonyl group  
508 coordinates to metal which may be due to strong electron withdrawing property of aryl group.  
509 Chemosensitivity activity of the complexes carried out against HCT-116 cancer cell line  
510 displayed that some of the complexes are cytotoxic. Of these, complex **3** was the most potent and  
511 whilst its potency was less than cisplatin, its selectivity for cancer as opposed to non-cancer cell  
512 lines in vitro was comparable to cisplatin. Further we have carried out the antibacterial studies  
513 performed against four pathogenic bacteria viz., *S. aureus*, *E. coli*, *B. thuringiensis* and *P.*  
514 *aeruginosa* but none of the compounds showed any activity. The complexes were fully  
515 characterized by various spectroscopic studies and their molecular structures were established by  
516 single X-ray analysis.

#### 517 *Acknowledgements*

518 Agreed Lapasam thanks CSIR- HRDG Delhi, India for providing financial assistance in  
519 the form of JRF fellowship. We express our sincere thanks to Dr. Krishna Mohan Poluri, IIT  
520 Roorkee for their help to carry out the antibacterial studies. We thank DST-PURSE SCXRD,  
521 NEHU-SAIF, Shillong, India for providing Single crystal X-ray analysis and other spectral  
522 studies.

#### 523 *Supplementary material*

524 CCDC 1874292 (2), 1874293 (3), 1874294 (4), 1874295 (5), 1874296 (7), 1874297  
525 (8), 1874298 (10), 1874299 (16), contains the supplementary crystallographic data for this paper.  
526 These data can be obtained free of charge via [www.ccdc.cam.ac.uk/data\\_request/cif](http://www.ccdc.cam.ac.uk/data_request/cif), by e-

527 mailing [data\\_request@ccdc.cam.ac.uk](mailto:data_request@ccdc.cam.ac.uk), or by contacting The Cambridge Crystallographic Data  
528 Centre, 12, Union Road, Cambridge CB2 1EZ, UK; Fax: +44 1223 336033.

## 529 References

- 530 [1] B. Rosenberg, L. VanCamp, J. E. Trosko, V. H. Mansour, *Nature*, 222 (1969) 385.
- 531 [2] F. Muggia, *Gynecol. Oncol.*, 112 (2009) 275.
- 532 [3] B. Rosenberg, *Adv. Exp. Med. Biol.*, 91 (1997) 129.
- 533 [4] R. Bieda, I. Ott, M. Dobroschke, A. Prokop, R. Gust, W.S. Sheldrick, *J. Biol. Inorg.*  
534 *Chem.*, 103 (2009) 698.
- 535 [5] Z. Liu, P.J. Sadler, *Acc. Chem. Res.*, 47 (2014) 1174.
- 536 [6] B.S. Murray, M.V. Babak, C.G. Hartinger, P.J. Dyson, *Coord. Chem. Rev.*, 306 (2016)  
537 86.
- 538 [7] J. Reedijk, *Platinum Met. Rev.*, 52 (2008) 2.
- 539 [8] [E. S. Antonarakis, A. Emadi. \*Cancer Chemother Pharmacol\* 66 \(2010\) 1.](#)
- 540 [9] [G. Süß-Fink, \*Dalton Trans.\*, \(2010\) 1673.](#)
- 541 [10] F.A. Khan, B. Therrien, [G. Süß-Fink](#), O. Zava, P.J. Dyson, *J. Organomet Chem.* 730  
542 (2013) 49-56.
- 543 [11] (a) [M. Haghdoost, J. Guard, G. Golbaghi, A. Castonguay, \*Inorg Chem.\*, 57 \(2018\) 7558.](#)  
544 (b) [E. Alessio, \*Eur. J. Inorg. Chem.\*, \(2017\) 1549.](#)
- 545 [12] [S. Thota, D. A. Rodrigues, D. C. Crans, E. J. Barreiro, \*J. Med. Chem.\*, 61 \(2018\) 5805.](#)
- 546 [13] [S. J. Lucas, R. M. Lord, A. M. Basri, S. J. Allison, Roger M. Phillips, A. J. Blackera, P.](#)  
547 [C. McGowan, \*Dalton Trans.\*, \(2016\) 6812.](#)
- 548 [14] [R. K. Gupta, R. Pandey, G. Sharma, R. Prasad, B. Koch, S. Srikrishna, P. Li, Q. Xu, D. S.](#)  
549 [Pandey. \*Inorg. Chem.\*, 52 \(2013\) 3687.](#)

- 550 [15] M. Melchart, A. Habtemariam, O. Novakova, S.A. Moggach, F.P.A. Fabbiani, S.  
551 Parsons, V. Brabec, P.J. Sadler, *Inorg. Chem.*, 46 (2007) 8950.
- 552 [16] M.A. Scharwitz, I. Ott, Y. Geldmacher, R. Gust, W.S. Sheldrick, *J. Organomet. Chem.*,  
553 693 (2008) 2299.
- 554 [17] S.K. Singh, S. Joshi, A.R. Singh, J.K. Saxena, D.S. Pandey, *Inorg.Chem.*, 46 (2007)  
555 10869.
- 556 [18] S. Blanck, J. Maksimoska, J. Baumeister, K. Harms, R. Marmorstein, E. Meggers,  
557 *Angew. Chem. Int. Ed.*, 51 (2012) 5244.
- 558 [19] S.P. Mulcahy, E. Meggers, *Med. Organomet Chem.*, Springer, 32 (2010) 141.
- 559 [20] S. Mollin, R. Riedel, K. Harms, E. Meggers, *J. Inorg. Biochem.* 148 (2015) 11.
- 560 [21] C. Kunick, I. Ott, *Angew. Chem. Int. Ed.*, 49 (2010) 5226.
- 561 [22] N. Gunasekaran, P. Ramesh, M.N.G. Ponnuswamy and R. Karvembu, *Dalton Trans.*,  
562 (2011) 12519.
- 563 [23] R.S. Correa, K.M. de Oliveira, F. G. Delolo, A. Alvarez, R. Mocoelo, A.M. Plutin, M.R.  
564 Cominetti, E. E. Castellano, A.A. Batista, *J. Inorg Biochem.* 150 (2015) 63.
- 565 [24] A. Mahajan, S. Yeh, M. Nell, C.E.J. van Rensburg, K. Chibale, *Bioorg. Med. Chem.*  
566 *Lett.* 17 (2007) 5683.
- 567 [25] W.S.I. Lin, C.N. Lok, K.Yan and C.M. Che, *Chem. Commun.*, 49 (2013) 3297.
- 568 [26] R.D. Campo, J.J. Criado, R. Gheorghe, F.J. Gonzalez, M.R. Hermosa, F. Sanz, J.L.  
569 Manzano, E. Monte, E.R. Fernandez, *J. Inorg. Biochem.* 98 (2004) 1307.
- 570 [27] Z.H. Li, Y. Zhang, Z.H. Peng, Y.G. Wang, *Huaxueshiji* 24 (2002) 214.
- 571 [28] N. Selvakumaran, N.S.P. Bhuvanesh, A. Endo and R. Karvembu, *Polyhedron*, 75 (2014)  
572 95.

- 573 [29] N. Selvakumaran, N.S.P. Bhuvanesh and R. Karvembu, Dalton Trans., (2014) 16395.
- 574 [30] K. Jeyalakshmi, J. Haribabu, N.S.P. Bhuvanesh, R. Karvembu, Dalton Trans., (2016)  
575 12518.
- 576 [31] S. Saeed, N. Rashid, P.G. Jones, M. Ali, R. Hussain, Eur. J. Med. Chem., 45 (2010) 1323.
- 577 [32] M. Kalidasan, R. Nagarajaprakash, M.R. Kollipara, Trans. Met. Chem., 40 (2015) 531.
- 578 [33] M. Kalidasan, R. Nagarajaprakash, S. Forbes, Y. Mozharivskyj, M.R. Kollipara, Z.  
579 Anorg. Allg. Chem., 641 (2015) 715.
- 580 [34] (a) S. Adhikari, O. Hussain, R.M. Phillips, W. Kaminsky, M.R. Kollipara, Appl.  
581 Organomet. Chem., 32 (2018) e4362. (b) S. Adhikari, O. Hussain, R.M. Phillips, W.  
582 Kaminsky, M.R. Kollipara, Appl. Organomet. Chem., 32 (2018) e4476.
- 583 [35] I.L. Mawnai, S Adhikari, W. Kaminsky, M.R. Kollipara, J. Organomet. Chem., 869  
584 (2018) 26.
- 585 [36] (a) M.A. Bennett, T.N. Huang, T.W. Matheson, A.K. Smith, S. Ittel, W. Nickerson,  
586 Inorg. Synth. 21(1982) 74.
- 587 [37] (a) G.M. Sheldrick, Acta Crystallogr. Sect.A, 46 (1990) 467.  
588 (b) G.M. Sheldrick, Acta Crystallogr. Sect.A, 64 (2008) 112.
- 589 [38] L.J. Farrugia, J. Appl. Crystallogr., 32 (1999) 837.
- 590 [39] (a) R.M Phillips, P.B. Hulbert, M.C. Bibby, N.R. Sleight, J.A. Double. Br J, Cancer. 65  
591 (1992) 359.
- 592 (b) S. Adhikari, D. Sutradhar, S.L. Shepherd, R.M. Phillips, A.K. Chandra, M. R.  
593 Kollipara, Polyhedron 117 (2016) 404.
- 594 [40] K. Jeyalakshmi, J. Haribabu, C. Balachandran, N.S.P. Bhuvanesh, N. Emi, R. Karvembu,  
595 New. J. Chem., 41 (2017) 2672.

596 [41] S. Adhikari, W. Kaminsky, M.R. Kollipara J. Organomet. Chem. 848 (2017) 95.

597

598 **Table 1.** Selected bond lengths (Å) and bond angles (°) of complexes

Complexes	<b>2</b>	<b>3</b>	<b>4</b>	<b>5</b>	<b>7</b>	<b>8</b>
Bond distances (Å)						
M(1)-CNT	1.787	1.778	1.672	1.689	1.665	1.784
M(1)-Cl(1)	2.413(1)	2.423(1)	2.426(1)	2.440(1)	2.4338(5)	2.4253(9)
M(1)-Cl(2)	2.427(1)	2.410(2)	2.406(1)	2.425(9)	2.4319(7)	2.411(1)
M(1)-S(1)	2.395(1)	2.370(2)	2.418(1)	2.366(1)	2.4004(7)	2.3857(8)
C=S(1)	1.689(9)	1.694(6)	1.703(5)	1.688(3)	1.695(2)	1.691(3)
Bond Angles (°)						
Cl(2)- M(1)-Cl(1)	90.52(4)	88.48(5)	88.87(5)	92.75(3)	87.67(2)	90.55(3)
S(1)- M(1)- Cl(1)	94.09(4)	91.47(5)	89.58(5)	92.34(3)	92.22(2)	92.69(3)
S(1) -M(1)-Cl(2)	92.56(4)	93.735	90.57(5)	92.41(3)	91.28(2)	92.73(3)

599

600 **Table 2.** Selected bond lengths (Å) and bond angles (°) of complexes

Complexes	<b>10</b>	<b>16</b>	<b>17</b>
Bond distances (Å)			
M(1)-CNT	1.675	1.678	1.784
M(1)-N(1)	2.138(2)	2.152(3)	2.161(3)
M(1)-N (azide)	2.127(4)	2.107(4)	2.125(5)
M(1)-S(1)	2.399(1)	2.406(1)	2.398(2)
C=S	1.713(3)	1.711(4)	1.723(4)
C=O	1.220(4)	1.229(5)	1.240(6)
Bond angle (°)			
N(1)-M(1)-N (azide)	85.7(1)	87.1(1)	90.7(2)
N(1)-M(1)-S(1)	67.27(7)	65.86(9)	67.0(1)
N(azide)-M(1)-S(1)	87.6(1)	88.8(1)	92.4(1)

601  
 602  
 603 **Table 3.** Response of HCT-116 (human colon cancer) and ARPE-19 to complexes **1-9** and  
 604 cisplatin. Each IC<sub>50</sub> value represents the mean ± standard deviation from three independent  
 605 experiments. The IC<sub>50</sub> selectivity index is defined as the mean IC<sub>50</sub> for ARPE-19 cells divided by  
 606 the mean IC<sub>50</sub> for HCT-116 cells with values greater than 1 representing selective cell kill in  
 607 cancer cells compared to non-cancer cells.

608

Compounds	IC <sub>50</sub> (μM)		
	HCT-116	ARPE-19	Selectivity Index
Complex 1	52.936 ± 4.815	33.515 ± 1.244	0.633
Complex 2	63.182 ± 1.916	36.604 ± 1.056	0.579
Complex 3	<b>35.172 ± 1.175</b>	37.941 ± 0.964	<b>1.078</b>
Complex 4	43.751 ± 2.480	36.744 ± 0.159	0.838
Complex 5	>100	80.267 ± 1.210	n/a
Complex 6	>100	78.252 ± 1.501	n/a
Complex 7	75.215 ± 4.733	46.913 ± 2.048	0.623
Complex 8	>100	>100	n/a
Complex 9	78.211 ± 8.658	69.301 ± 1.606	0.886
Cisplatin	2.78 ± 1.40	3.43 ± 0.48	1.233

609